Solar Energy 227 (2021) 477–489

Contents lists available at ScienceDirect

Solar Energy

journal homepage: www.elsevier.com/locate/solener

Inactivation of simulated aquaculture stream bacteria at low temperature using advanced UVA- and solar-based oxidation methods

Elena Villar-Navarro [a,*], Irina Levchuk [b,c,*], Juan José Rueda-Márquez [b], Tomáš Homola [d], Miguel Ángel Moriñigo [e], Riku Vahala [c], Manuel Manzano [a]

[a] Department of Environmental Technologies, INMAR-Marine Research Institute, Faculty of Marine and Environmental Sciences, University of Cadiz, Polígono Rio San Pedro s/n, Puerto Real, 11510 Cadiz, Spain
[b] Fine Particle and Aerosol Technology Laboratory, Department of Environmental and Biological Sciences, University of Eastern Finland, P.O. Box 1627, FI-70211 Kuopio, Finland
[c] Water and Environmental Engineering Research Group, School of Engineering, Aalto University, P.O. Box 15200, FI-00076 Aalto, Finland
[d] Department of Physical Electronics, Faculty of Science, Masaryk University, Kotlářská 267/2, 611 37 Brno, Czech Republic
[e] Department of Microbiology, Faculty of Sciences, University of Málaga, 29071 Málaga, Spain

ARTICLE INFO

Keywords:
Aquaculture streams
UVA-based AOPs
Solar AOPs
Low temperature

ABSTRACT

In this work the effect of water temperature (6 ± 1 °C and 22 ± 1 °C) on inactivation of bacteria (10^4 –10^6 CFU mL^{-1}; *Pseudomonas* spp., *Aeromonas spp*. and *Enterobacter* spp.) in simulated aquaculture streams (SAS) using UVA based advanced oxidation processes (AOP) (H_2O_2-assisted UVA; photocatalysis; H_2O_2-assisted photocatalysis) and solar driven AOPs (H_2O_2-assisted solar disinfection, SODIS) was studied. Efficiency at 22 °C in terms of inactivation rate was higher using H_2O_2-assisted photocatalysis (H_2O_2/UVA-TiO_2/polysiloxane) > H_2O_2-assisted UVA disinfection (UVA/H_2O_2 – 10 mg L^{-1}) > photocatalysis (UVA-TiO_2/polysiloxane) > UVA disinfection. At low temperature (6 °C) the inactivation rate increased with SODIS/H_2O_2 > SODIS > H_2O_2-assisted UVA disinfection (UVA/H_2O_2 – 10 mg L^{-1}) > H_2O_2-assisted photocatalysis (H_2O_2/UVA-TiO_2/polysiloxane) > photocatalysis (UVA-TiO_2/polysiloxane). The main results indicate that the inactivation rates increased when hydrogen peroxide (10 mg L^{-1}) was used during H_2O_2-assisted UVA disinfection and photocatalysis. In addition, exposure of SAS to hydrogen peroxide for 24 h (in absence of light) at room temperature decreased the subsequent exposure UVA irradiation dose by almost four times.

Drastic increase of inactivation rate was observed at low water temperature (6 ± 1 °C) when UVA- and solar-based AOPs were employed compared to 22 ± 1 °C. The treatment with SODIS proved to be more effective in Finland than in Spain. The effect of the low temperature (6 ± 1 °C) was proposed as a critical factor during UVA disinfection (UVA/H_2O_2 and photocatalysis) that can increase the disinfection rate constant (k_{max}) by 1.3–5.2 times, leading to a reduction of the treatment costs (€ m^{-3}) by 1.3–3.3 times. The mechanism of observed enhanced disinfection at low water temperature (6 ± 1 °C) when natural solar light and UVA are employed as irradiation sources for UVA/H_2O_2 and photocatalytic bacteria inactivation was proposed. No regrowth was observed in case of H_2O_2-assisted AOPs.

1. Introduction

In 2018, the Food and Agriculture Organization of the United Nations (FAO) published official statistics on fisheries and aquaculture highlighting that global fish production reached 171 million tonnes, 47% of which comes from aquaculture. Taking into consideration that world capture fisheries production has been stabilized, aquaculture has to take responsibility for achieving the production targets that the world's population requires. This implies that world aquaculture production will continue to increase every year. For instance, the aquaculture production reached 110.2 million tons in 2016 with a value of 243 500 million USD (FAO, 2018).

* Corresponding authors at: Department of Environmental Technologies, INMAR-Marine Research Institute, Faculty of Marine and Environmental Sciences, University of Cadiz, Polígono Rio San Pedro s/n, Puerto Real, 11510 Cadiz, Spain. Fine Particle and Aerosol Technology Laboratory, Department of Environmental and Biological Sciences, University of Eastern Finland, P.O. Box 1627, FI-70211 Kuopio, Finland.
E-mail addresses: elena.villar@uca.es (E. Villar-Navarro), irina.levchuk@uef.fi (I. Levchuk).

https://doi.org/10.1016/j.solener.2021.09.029
Received 17 December 2020; Received in revised form 5 September 2021; Accepted 10 September 2021
Available online 20 September 2021

Aquaculture systems can be classified according to different parameters (Soltan, 2016) such as water exchange (open, flow-through or recirculating system). In the case of recirculating systems, e.g. recirculated aquaculture systems (RAS), the water flows through a closed system and the growth of the fish takes place under controlled conditions (e.g. pH, salinity or oxygenation). The use of water in RAS is very low compared to other systems like flow-through, the discharge of contaminated water is also lower while production yields can be higher (Dauda et al., 2019). Therefore, RAS is increasingly developed and postulated as one of the best options to meet the future demand for fish worldwide (Edwards, 2015; Ranjan et al., 2019).

Regulation of organic matter, nitrogen species, dissolved gases, pH, alkalinity, salinity and pathogenic organisms is required in order to ensure proper operation of RAS. Pathogens are of high concern in RAS due to risk of infection of fish and other reared organisms such as mollusks or crustaceans. The most studied target bacterial genus in aquaculture are *Vibrio, Aeromonas, Pseudomonas, Flavobacterium and Lactococcus* (Culot et al., 2019). The most commonly used technologies for water disinfection in RAS are UVC treatment (Sharrer et al., 2005), chlorination (Ben-Asher et al., 2019), ozonation (Davidson et al., 2011), disinfection with peracetic acid (Liu et al., 2016) and/or hydrogen peroxide (Schmidt et al., 2006). The challenges faced by fish farms using these technologies are related to energy use, cost of chemicals and possible toxicity of chemicals to fish or other reared organisms (Badiola et al., 2018; Chhetri et al., 2019). This can decrease the profitability and increase the costs and carbon footprint of aquaculture production.

During the last decades, alternative and environmentally friendly disinfection technologies are emerging, such as AOPs and SODIS. AOPs are promising techniques for disinfection of various water matrices (Levchuk et al., 2019, 2018; You et al., 2019). Among main advantages of AOPs are absence of solid waste generation (for majority of AOPs) and its non-selectivity. However, there is scarce information on the disinfection of aquaculture waters/streams. In fact, almost in all studies focused on the disinfection of aquaculture waters the UVC lamps were used (Jorquera et al., 2002; Kasai et al., 2002; Summerfelt et al., 2009; Torgersen & Håstein, 1995). The main disadvantages of traditional UV lamps include capital, operational and maintenance costs, contamination risk due to mercury residues and short lifetime (Prasad et al., 2020). An alternative to traditional UV lamps and more environmentally friendly source of artificial irradiation is light-emitting diodes (LEDs). In comparison with conventional UV lamps LEDs have a longer life time, do not contain toxic elements, have compact size and are more energy efficient (Chang et al., 2012). Only a few studies have reported application of LEDs-based disinfection methods for inactivation of pathogens in aquaculture streams using UVA (Qi et al., 2020) and UVC LEDs (Moreno-andrés et al., 2020). Thus, it is important to study feasibility of LEDs as irradiation source for water treatment and disinfection of aquaculture water (Song et al., 2016).

SODIS is widely studied in the field of wastewater and drinking water treatment (Figueredo-Fernández et al., 2017; Giannakis et al., 2016; Zhang et al., 2018), but its viability for aquaculture water is not well established. The effect of water temperature on SODIS has been studied and synergistic effects at water temperatures above 45 °C was reported by many researchers (Giannakis et al., 2014; Joyce et al., 1996; McGuigan et al., 1998). Interestingly, an antagonistic effect of temperature in the range 30 – 40 °C was suggested recently (Giannakis et al., 2014; Vivar et al., 2017). In addition, the combination of UVA irradiation along with hydrogen peroxide can possibly generate damage of DNA and cellular proteins that leads to a total inactivation of high concentrations of bacteria (Hamamoto et al., 2007; Villar-Navarro, Levchuk, Rueda-Márquez, & Manzano, 2019).

However, to the best of our knowledge, there are no studies at lower water temperatures (below 10 °C), which are typical in different climatic zones (e.g. Nordic countries, North of India, etc.). Taking into consideration that many aquaculture systems are located in Nordic countries, the effect of lower temperatures on disinfection using UVA- and solar-based AOPs may be of particular interest for practical applications. A step forward was taken in this study and effect of low water temperature (6 ± 1 °C) on inactivation efficiency of target bacteria in simulated aquaculture streams using UVA- and solar-based AOPs as alternative and environmentally friendly irradiation sources was studied. These technologies were also compared at water temperatures of 6 and 22 °C. Regrowth of target bacteria have studied after 24 h for all tested technologies. Operational costs of studied disinfection methods were evaluated.

2. Material and methods

2.1. Water matrix

The water for experiments was taken from the Gulf of Finland, the location of sampling point is shown in Fig. 1. Taking into account that concentration of bacteria in natural brackish water was relatively low (~10^2 CFU mL^{-1}) yeast was added in order to reach concentration of target bacteria representative for aquaculture streams (10^4 – 10^6 CFU mL^{-1}). Before each experiment brackish water was first filtered through 1.6 μm and, after 5 mg $L^{-1}$of yeast was added, water was kept at 37 °C during 24 h. During preservation of brackish water with yeast at 37 °C the bottles were slightly opened for gas exchange.

After testing how addition of various concentrations of yeast (5 mg L^{-1} – 100 mg L^{-1}) affect bacteria growth, the optimum yeast concentration was selected. The main criteria for selecting optimal yeast concentration were *(i)* leading to high concentrations of bacteria, *(ii)* does not lead to increase of the total organic carbon (TOC). Thus, concentration of 5 mg L^{-1} was chosen as an optimal (Figure S1). Bacteria concentration after yeast addition was in the range of 10^4 – 10^6 CFU mL^{-1}, which is representative values for RAS stream as described in the literature (de la Pena et al., 2001; Suantika et al., 2018). As it is fresh water, the final concentration of bacteria depends on the water sampled. The physic-chemical characterization of natural brackish water and simulated aquaculture stream (SAS) are shown in Table 1. The transmittance of SAS was measured after increasing the concentration of target bacteria in the range 280 – 400 nm. It should be noted that in all cases the transmittance was higher than 90%.

Bacteria present in the SAS were isolated using TCBS agar. Growth of green, yellow and orange colonies was observed (Figure S2). Green colonies were identified with the genus *Pseudomonas* sp. (98 – 99% similarity) and the yellow colonies with the species *Aeromonas salmonicida* (97% similarity). The less frequent isolated colonies (orange) were identified as *Aeromonas veronii* (98% similarity) and *Enterobacter cloacae* (98%). Further information about bacterial strains is presented in Table S1. The three genus, *Pseudomonas, Aeromonas* and *Enterobacter* have not been identified precisely as pathogenic bacteria, although are of interest in aquaculture, as they have been reported as pathogenic bacteria for fish and invertebrates and have a negative impact on aquaculture production (Culot et al., 2019; Gao et al., 2016; Gonçalves Pessoa et al., 2019; Zepeda-Velázquez et al., 2017).

2.2. Preparation and characterization of TiO_2/polysiloxane thin films

AOPs for photocatalytic inactivation of pathogens in the water was supported by nanocomposite TiO_2/polysiloxane coatings prepared by means of material printing technique using inkjet printer Fujifilm Dimatix 283. The photocatalytic activity was the composite was demonstrated in (Homola et al., 2016), and the coatings also show a great promise in other solar energy-related applications such as thin-film perovskite solar cells (Homola et al., 2020a). Thin films were printed on flexible polyethylene terephthalate (PET) substrate, and the advantage of this method lies in the possibility to produce photocatalyst on large-scale (hundreds square m^2 by roll-to-roll manufacture), and thus represents a low-cost approach for AOPs supported water disinfection. The printable ink was created from the dispersion (6 mL) of TiO_2

Fig. 1. Map (left) and photo (right) of the sampling point and 1 L plastic bottles used at Gulf of Finland (Espoo, Finland).

Table 1
Physico-chemical characterization of the tested water before (without filtration) and after filtration and the addition of yeast (simulated aquaculture stream) and stored in dark at 37 °C. Mean value and standard deviation.

Parameter	Before addition of yeast	After addition of yeast
TDN (mg L^{-1})	0.3 ± 0.2	0.8 ± 0.2
TDP (μg L^{-1})	38 ± 1	80 ± 1
COD (mg L^{-1})	7.7 ± 0.1	8.7 ± 0.3
TOC (mg C L^{-1})	7.1 ± 0.6	8.2 ± 0.2
Conductivity (mS cm^{-1})	10.2 ± 1.9	9.8 ± 1.2
Salinity (‰)	4.9 ± 0.1	4.9 ± 0.1
pH	7.7 ± 0.4	8.0 ± 0.2
Hardness (mmol L^{-1})	9.7 ± 0.3	9.8 ± 0.1
Transmittance (365 nm, %)	87 ± 4	96 ± 1
Fe (μg L^{-1})	13.7 ± 0.7	13.7 ± 0.7
Ti (μg L^{-1})	5.4 ± 0.3	5.4 ± 0.3
CFU mL^{-1}	91 ± 12	$7{\cdot}10^4 - 2{\cdot}10^6$

nanoparticles (Evonik Aeroxide P25) in Dowanol PM (20 wt%) and mixed with siloxane binder (20 wt% in anhydrous ethanol) and isobutanol (8 mL). Then, about two cm^3 of glass balls (1 mm) were added to prepared ink and left overnight on an oscillating shaker (1000 rpm). Final ink solution with TiO_2:Siloxane ratio of 75:25 was then used for printing of thin films as reported elsewhere (Homola et al., 2016; Levchuk et al., 2019). The thickness of printed films was about 300 nm.

Scanning electron microscopy (Nova NanoSEM 450) and atomic force microscopy (AFM, Ntega Prima NT-MDT) were used to examine the morphology of printed TiO_2/polysiloxane thin films. Bonding state of printed coatings was evaluated by means of Horriba LabRAM HR Evolution microraman spectrometer with 532-nm laser.

Water contact angle of TiO_2/polysiloxane thin films was measured using OCA 15plus connected to digital camera (NEURTEK Instruments). The 5 μL droplets of Milli-Q water were placed on the surface of TiO_2/polysiloxane coatings before photocatalytic experiments. Three measurements were performed and mean values were evaluated.

2.3. Experimental procedures for disinfection of simulated aquaculture stream

2.3.1. Experimental procedure for UVA-based AOPs

The H_2O_2-assisted UVA experiments were performed in batch operation using a glass reactor filled with 1200 mL of simulated aquaculture stream. Continuous magnetic stirring was applied during all experiments (Fig. 2A). The height of the water column was 8.5 cm. The distance between the water surface and the irradiation source was 1 cm. The UVA-LEDs (365 nm) were used as irradiation source. The UVA irradiance on the surface of the water (46.5 ± 0.6 W m^{-2}) was measured using UV AB Light Meter (General UV513AB). The zero point of the experiment coincides with addition of H_2O_2 and switching on the UVA. Experiments were conducted for 3 h and samples were taken after 0, 15, 35, 55, 90, 120, 180 min. During the experiments, two to three dilutions were analysed in each sample in duplicate. Colonies were counted

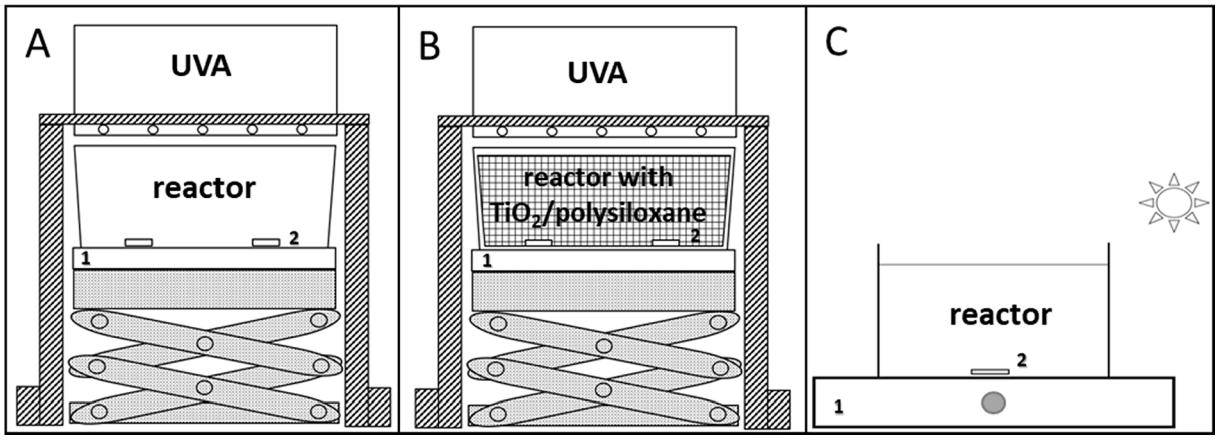

Fig. 2. Schematic representation of the experimental set-up. A. UVA-LEDs set-up; B. UVA-LEDs set-up using TiO_2/polysiloxane photocatalyst; C. SODIS set-up. Magnetic stirrer is marked as (1) and stirring bar as (2) in A – C.

(maximum 150 CFU per plate) using a colony counter (ColonyStar, Funke Gerber). After each disinfection experiment, SAS samples were stored at room temperature in absence of light for 24 h in order to check bacteria regrowth. Bacteria were cultivated using TCBS according to the procedure described above. The UVA/H_2O_2 disinfection tests were performed at 22 ± 1 °C (room temperature) and 6 ± 1 °C. Once the SAS sample was taken out of the oven, it was cooled down until the water reached room temperature (22 ± 1 °C). All low temperature experiments were conducted in a controlled cold room with a fixed temperature of 6 ± 1 °C. The experiment started in all cases when the water reached 6 °C. The water temperature was measured with a mercury thermometer.

Photocatalytic experiments were conducted with the same experimental set-up (Fig. 2B). Photocatalytic thin films, which were prepared as described in *section 2.2.*, were attached to the walls and bottom of the reactor. The total geometrical area of immobilized photocatalyst was ~ 0.45 cm^2 mL^{-1}. The SAS sample was magnetically stirred during 0.5 h in dark after being exposed to UVA in order to test the bacterial adhesion to the photocatalyst. Experiments on H_2O_2-assisted photocatalytic disinfection were conducted as photocatalytic tests except that H_2O_2 was added in the beginning of each run.

2.3.2. Experimental procedure for solar-based AOPs

Solar disinfection experiments were conducted in Pyrex glass reactor without recirculation (Fig. 2C) in order to simulate the central section of an open channel raceway (Villar-Navarro et al., 2019). The SODIS experiments, with and without hydrogen peroxide, were carried out at the same time using two identical reactors. The volume, height of the water column and internal diameter of the reactor were 3500 mL, 10 cm and 22.5 cm, respectively. All experiments were performed under continuous magnetic stirring for 3 h and samples were taken after 0, 15, 35, 55, 90, 120, 180 min. The ambient and water temperature during solar experiments was 6 ± 1 °C as the experiments were performed during autumn in Finland. Global UV radiometer (CUV 5, Kipp & Zonnen, the Netherlands) was used (range 280 – 400 nm) in order to measure the irradiance. Data of UV irradiation are expressed as UV dose (Wh m^{-2}). After disinfection experiment, SAS samples were stored during 24 h in absence of light at room temperature in order to check possible bacteria regrowth. Bacteria were cultivated using TCBS according to the procedure described above.

2.4. Analytical methods

2.4.1. Chemical analysis

Concentration of hydrogen peroxide in water was measured spectrophotometrically using cobalt carbonate method (absorption was measured at 260 nm) (Masschelein et al., 1977). Transmittance (λ = 365 nm) of the water was monitored using UV–Visible spectrophotometer UV-1800 Shimadzu. Conductivity and salinity of SAS were measured using conductivity meter Orion 101. Determination of pH was carried out using inoLab 7110 pH-meter. Total dissolved nitrogen (TDN), total dissolved phosphorus (TDP), chemical oxygen demand (COD) and hardness was measured according to standard methods (APHA, WEF, AWWA, 2018b). Total organic carbon (TOC) was analyzed as non-purgeable organic carbon using a TOC-V_{CSH} analyzer (Shimadzu, Japan). Concentration of dissolved titanium and iron in SAS before and after experiments was measured by means of inductively coupled plasma-mass spectrometry (ICP-MS), Thermo Elemental.

2.4.2. Microbiological analysis and identification

TCBS (Thiosulfate Citrate Bile Salts Sucrose Agar) agar was used as culture media for target bacteria. Membrane filtration method (APHA, WEF, AWWA, 2018a) was employed for detection and enumeration of bacteria. Serial dilutions were carried out to quantify high concentrations of bacteria. The isolated colonies (Figure S2) were identified through a partial sequencing of 16S rRNA gene according to previously described procedure (Levchuk et al., 2019). The UV dose (Wh m^{-2}) was estimated according to Eq. (1).

$$D_{UV} = I_t \cdot \Delta t \quad (1)$$

where I_t is the UVA irradiance (W m^{-2}) and Δt is the time between taking samples (h).

2.4.3. Data analysis

Results of bacteria inactivation were fitted to three different models, namely: ″Log-linear″ (Eq. (2)), ″Log-linear + shoulder″ (Eq. (3)) and ″Log-linear + tail″ (Eq. (4)). The experimental results were modelled using the GinaFit tool (Geeraerd et al., 2005) and data were validated using the coefficient of determination (R^2).

$$N_D = N_0 \bullet e^{(-k_{max} \cdot D_{UV})} \quad (2)$$

$$N_D = N_0 \bullet e^{(-k_{max} \cdot D_{UV})} \bullet \frac{e^{(k_{max} \cdot SL)}}{1 + (e^{(k_{max} \cdot SL)} - 1) \bullet e^{(k_{max} \cdot D_{UV})}} \quad (3)$$

$$N_D = (N_0 - N_{res}) \bullet e^{(-k_{max} \cdot D_{UV})} + N_{res} \quad (4)$$

in which N_D is bacteria concentration at a certain dose (CFU mL^{-1}), N_0 is initial bacterial concentration (CFU mL^{-1}), D_{UV} is applied irradiation dose (Wh m^{-2}), k_{max} is disinfection rate constant (m^2 $W^{-1}h^{-1}$) and SL is shoulder length (Wh m^{-2}) and N_{res} is residual bacteria concentration (CFU mL^{-1}).

Bacterial regrowth was calculated according to Lindenauer & Darby (1994) as shown in Eq. (5):

$$\%Regrowth = \frac{N_r - N_t}{N_0 - N_t} \bullet 100\% \quad (5)$$

where N_0 is initial bacteria concentration (CFU mL^{-1}), N_t is bacterial concentration after a disinfection (CFU mL^{-1}) and N_r is reactivated bacteria after 24 h darkness (CFU mL^{-1}).

3. Results and discussion

3.1. UVA-based AOPs

3.1.1. Control tests

A control experiment was performed using UVA without adding hydrogen peroxide. The initial concentration of bacteria was $2.4 \cdot 10^5$ CFU mL^{-1}. No inactivation of bacteria was observed after 90 min exposure (70 Wh m^{-2}). After 180 min of exposure (140 Wh m^{-2}) the concentration was reduced by 19%. Therefore, the use of UVA is not sufficient to inactivate high concentrations of bacteria in short treatment times.

In order to study the effect of hydrogen peroxide on target bacteria, 24-hour tests were performed in dark using five different initial concentrations of H_2O_2: 0, 1, 2.5, 5, 10 and 15 mg L^{-1} (Figure S3). Taking into account that fresh brackish water was used for preparation of SAS water before each experiment, the average initial concentration of bacteria vary from 10^4 to 10^6 CFU mL^{-1}. In general, as the concentration of hydrogen peroxide increased, the concentration of bacteria decreased (Figure S3). Thus 60, 75, 92 and 98% of bacteria inactivation was achieved after 24 h when initial concentrations of H_2O_2 were 2.5, 5, 10 and 15 mg L^{-1}, respectively. Conversely, an increase in the bacteria concentration was observed when concentration of H_2O_2 was 1 mg L^{-1}.

The residual concentration of H_2O_2 after 24 h was 0.44 ± 0.04 mg L^{-1} when initial concentration of H_2O_2 of 1, 2.5 and 5 mg L^{-1} was used, while residual H_2O_2 was 7.71 ± 0.30 mg L^{-1} when initial H_2O_2 concentration was 10 and 15 mg L^{-1}. Regarding the water quality, in case the water is discharged into a receiving water body, it is not recommended that the concentration of H_2O_2 exceed 100 mg L^{-1}. No observable effect concentration (NOEC) was reported to occur from 10 to 1132 mg H_2O_2 L^{-1} for different freshwater fish. In case of RAS, acute toxicity was observed at concentrations above 37 mg H_2O_2 L^{-1} (Schmidt et al., 2006). It should be noted that toxicity strongly depends on the fish species and its development stage. Thus, disinfected water must contain the minimum

concentration of residual hydrogen peroxide before being either discharged into the environment or reused in a RAS, provided that a prior toxicity study is conducted.

Therefore, an increase of hydrogen peroxide concentration leads to a higher percentage of inactivation in absence of light, mostly within a period of contact time between 5 h and 24 h. It should be noted that elevated concentrations of hydrogen peroxide (2.5 – 15 mg L^{-1}) are required for cell damage to be effective so when the concentration of H_2O_2 increases the bacterial cell wall are also affected by weakening it and leading it to inactivation (Rincón & Pulgarin, 2006). These results may be attributed to the fact that major part of the hydrogen peroxide is spend for oxidation of organic matter present in the SAS (TOC = 8.2 mg L^{-1}).

3.1.2. *Inactivation of target bacteria using H_2O_2-assisted UVA disinfection*

The effect of initial H_2O_2 concentration on bacterial inactivation in simulated aquaculture stream by UVA/H_2O_2 process has been studied. The initial concentration of H_2O_2 varied from 2.5 mg L^{-1} to 15 mg L^{-1} (Fig. 3).

Bacterial inactivation was negligible when concentration of H_2O_2 was 2.5 mg L^{-1}. The residual concentration of H_2O_2 after 3 h was 2.2 mg L^{-1}. However, as the initial concentration of H_2O_2 increases (from 5 to 15 mg L^{-1}), so does the rate of bacteria inactivation (k_{max}) from 0.028 m^2 $W^{-1}h^{-1}$ (SL = 50.55, R^2 = 0.979, "Log-Linear + shoulder model") to 0.078 m^2 $W^{-1}h^{-1}$ (SL = 26.03; R^2 = 0.986, "Log-Linear + shoulder model"). The rest of the kinetic parameters can be found in Table S2.

Thus, the required UVA dose for reaching 4 Log Removal Value (LRV) decreased from 383 (494 min of contact time) to 145 Wh m^{-2} (188 min of contact time) with increase of H_2O_2 concentration from 5 to 15 mg L^{-1}.

It should be noticed that there was no differences in bacterial inactivation when 10 and 15 mg L^{-1} was used. Thus, initial concentration of H_2O_2 of 10 mg L^{-1} was selected as an optimal and was used in the following experiments. In this way, the lowest possible concentration of H_2O_2 leading to desired level of bacterial inactivation at the lowest possible dose would be used. At the same time relatively low residual H_2O_2 (>2.5 mg L-1) concentration after applied disinfection processes ensure absence of bacteria regrowth due to toxicity of H_2O_2 to target bacteria (as suggested in *section 3.1.*). After 24 h of storage at 22 °C, no bacterial regrowth was observed (0 CFU mL^{-1}) which ensures that disinfection is permanent.

A similar study was conducted by Feng et al. (2020): UVA lamps (40 W m^{-2}), 10 mg H_2O_2 L^{-1} and initial bacteria concentration of 10^6 CFU mL^{-1}. In that study a complete disinfection was obtained (0 CFU mL^{-1}) after a contact time of 90 min (60 Wh m^{-2}), which was less than that obtained in this study. The differences may be due to the sensitivity of the bacteria (stock of *Escherichia coli*) and the type of reactor (height: 55 mm).

An additional experiment was carried out to test how the inactivation rate can be affected in case the SAS is stored for 24 h with 10 mg L^{-1} hydrogen peroxide in absence of light prior to UVA disinfection (Figure S4). Results showed that after 24 h at room temperature (22 °C), the concentration of bacteria was reduced by 2 LRV to $1.4{\cdot}10^3$ CFU mL^{-1}. Then, UVA was switched on for 90 min. The disinfection rate constant (k_{max}) was 0.114 $W^{-1}h^{-1}$ m^{-2} (R^2 = 0.999, "Log-linear model"). After 15 min of treatment the concentration dropped to 70 CFU mL^{-1}, while after 60 min detection limit was reached. The dose for 4 LRV was 43.5 Wh m^{-2} (56 min of contact time), being the residual concentration of hydrogen peroxide 6.2 mg L^{-1}. Furthermore, regrowth was not observed after 24 h (0 CFU mL^{-1}). Therefore, a previous exposure of aquaculture streams to hydrogen peroxide increases sensitivity of bacteria to subsequent UVA treatment, reducing four times the dose needed to reach 4 LRV compared with UVA combined with 10 mg H_2O_2 L^{-1}. It should be noted that H_2O_2 (as one of reactive oxygen species - ROS) can inactivate microorganisms (Matthijs et al., 2012). However, the concentration of H_2O_2 required for suppression or killing microorganisms vary. For instance, the concentration of H_2O_2 in the range of 10^{-5} – 10^{-4} M (0.34 – 3.4 mg L^{-1}) was reported to be sufficient to supress the growth of cyanobacteria *Anacystis nidulans* and *Anabaena variabilis* in dialysis culture (Samuilov et al., 1999), while 100 mg L^{-1} of H_2O_2 was required to reach 99.99% of *Escherichia coli* strain ATCC 8739 inactivation (4 h) (Labas et al., 2008). Target bacteria used in this study were *Pseudomonas* sp., *Aeromonas salmonicida*, *Aeromonas veronii* and *Enterobacter cloacae*, all of which are known to have positive catalase test. Catalase protects microorganisms against oxidative stress of H_2O_2 by breaking it to water and oxygen (Srinivasa Rao et al., 2003). Thus, it can be expected that target bacteria in our study might be more resistant to oxidative stress produced by presence of H_2O_2 as it was demonstrated in earlier studies (Walczak & Swiontek Brzezinska, 2009). Based on observed effect of H_2O_2 on target bacteria after 24 h (2 LRV reduction) it can be assumed that the concentration of H_2O_2 used in this tests (10 mg L^{-1}) was sufficient to provide an oxidative stress, even though complete inactivation of target bacteria was not reached. Further addition of UVA allowed to reach 4 LRV faster due to the fact that target bacteria were under oxidative already during previous 24 h.

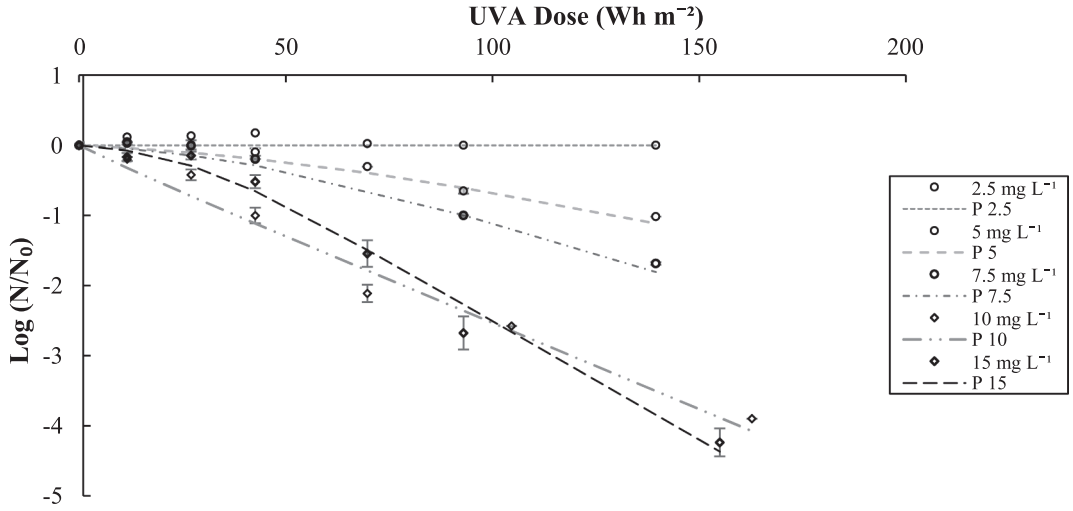

Fig. 3. Target bacteria inactivation in SAS using UVA/H_2O_2 disinfection under different H_2O_2 concentration (H_2O_2 concentrations varied from 2.5 to 15 mg L^{-1}, water temperature 22 °C, max. experimental time 180 – 210 min, which corresponds to UVA Dose 140 – 163 Wh m^{-2}). Symbols represents experimental data. Lines (P) represents predicted values of kinetic disinfection model.

3.2. Inactivation of target bacteria using UVA-based photocatalysis and H_2O_2 – Assisted photocatalysis

3.2.1. Characterization of printed TiO_2/polysiloxane thin films

The wettability of TiO_2/polysiloxane films was evaluated by contact angle measurement, which showed water contact angle of 125.6° ± 1.2°, indicating that the surface of the coating is hydrophobic. The wettability of the coating might play a role in the efficiency of the photocatalyst in direct contact with contaminants, e.g. hydrophilic coatings showed less efficiency, probably due to a thin layer of water present between photocatalyst and contamination which inhibits decomposition via direct electron or energy transfer (Levchuk et al., 2019).

Morphology of printed TiO_2/polysiloxane thin films was studied by means of SEM and AFM (Fig. 4 a and b).

Both SEM and AFM images confirmed good homogeneity of the coating with grainy features from TiO_2 nanoparticles embedded in a siloxane binder with the size of the grains ranging from 50 to 250 nm, which is in agreement with earlier reports (Homola et al., 2016). The surface of the coating was rough as AFM showed RMS roughness of approx. 120 nm.

The structure of the TiO_2/polysiloxane surface was further determined by Raman spectroscopy shown in Fig. 4 (c).

Presumably, the inkjet printing has no effect on the preferential crystalline orientation of TiO_2 grains, a map of 20 measurements was performed over the area 50 mm^2 to provide information on the homogeneity of the orientation of grains. All Raman spectra presented in Fig. 4c shows typical peaks characteristic for TiO_2 in anatase structure: Eg(1) at 139.4 cm^{-1}, Eg(2) at 197.2 cm^{-1}, B1g(1) at 395.3 cm^{-1}, A1g at 516.9 cm^{-1}, Eg(3) at 633.5 cm^{-1}. The intensity of the measured Raman spectra varied, confirming the random orientation of anatase grains within the polysiloxane binder forming TiO_2/polysiloxane mesoporous nanocomposite films. Fig. 4d shows a map of the intensity of the main anatase peak Eg(1) located at 139.4 cm^{-1}, related to the vibration of Ti atom from "left to right" within the anatase crystalline structure. The intensity of the peak varied from $1.2{\cdot}10^3$ to $1.7{\cdot}10^4$, which represent a difference of one order. Although Raman spectra in Fig. 4c do not clearly distingue between anatase and rutile phase in P25 TiO_2, similarly as recently shown in Ma et al. (2020), in our recent work (Homola et al., 2020) we showed that Evonik Aeroxide P25 nanoparticles consist of a small portion of rutile, which was observed in XRD spectra of a powder showing rutile peak (1 1 0). The composition of TiO_2 nanoparticles Aeroxide P25 from Evonik and the contribution of anatase, rutile and amorphous TiO_2 is comprehensively explained by Jiang et al. (2018), who analysed the microstructure of P25 nanoparticles and confirmed that Evonik Aeroxide P25 consists of individual anatase and rutile nanoparticles, combined with approximately 15 % of rutile formed heterojunction structure with anatase.

3.2.2. Photocatalytic disinfection

Photocatalytic disinfection tests were conducted using TiO_2/polysiloxane thin films (in absence and presence of H_2O_2) and inactivation of target bacteria was monitored on the course of the experiments. The

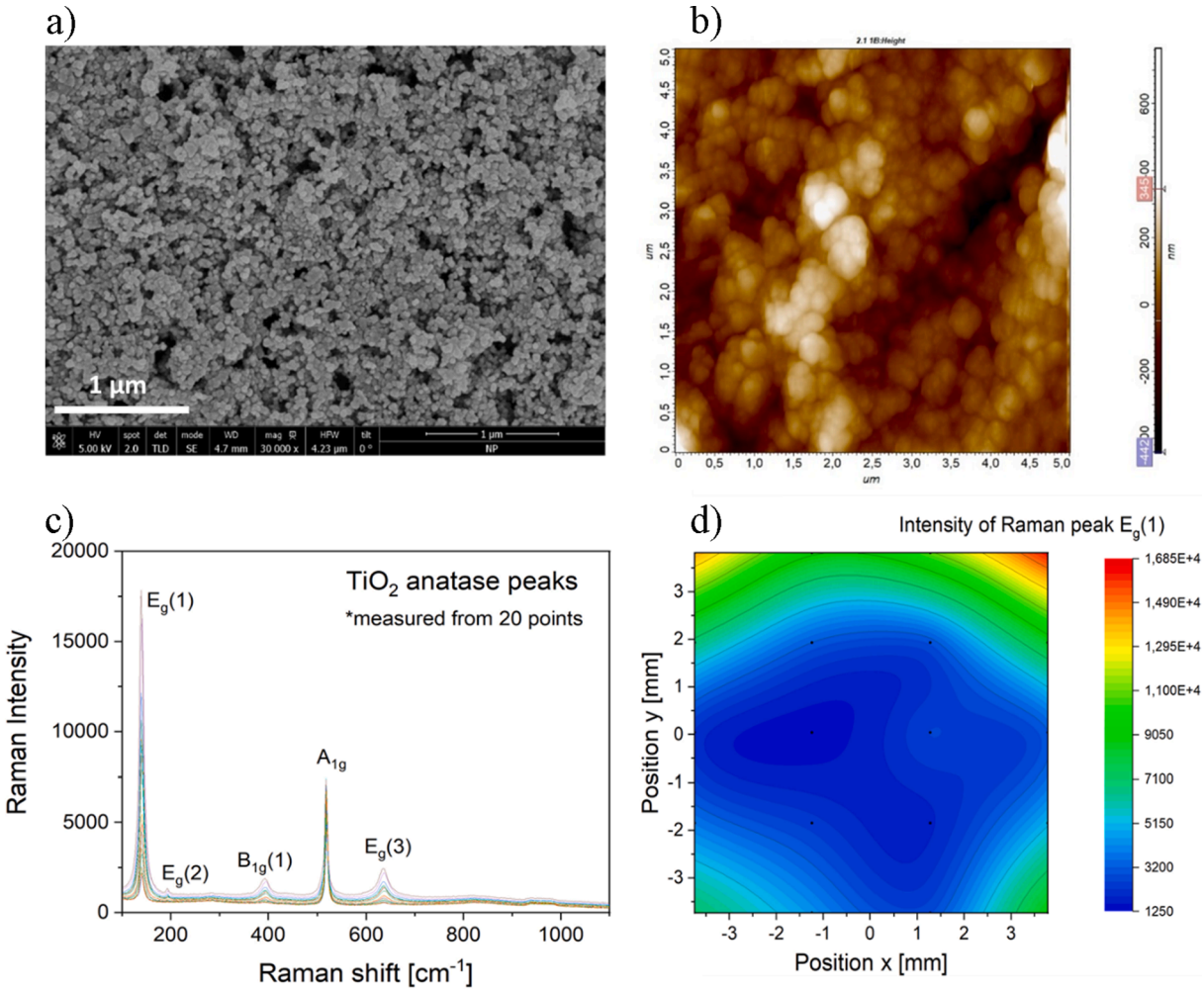

Fig. 4. a) SEM and b) AFM images of hydrophobic TiO_2/polysiloxane thin film printed on flexible PET substrate; c) Raman spectra for TiO_2/polysiloxane coating taken from 20 spots at area approx. 50 mm^2; d) spatial distribution of intensity in Raman Eg(1) peak corresponding to Fig. 4c.

UVA disinfection (in absence of photocatalyst and/or H_2O_2) and adhesion tests were performed as reference tests. Maximum duration of each experiment was 3.5 h. According to results obtained in our earlier study (Levchuk et al., 2018), hydrophobic TiO_2/polysiloxane coatings were more efficient for bacteria inactivation than hydrophilic TiO_2/SiO_2, in which the polysiloxane was converted into almost pure amorphous SiO_2 by the atmospheric ambient air plasma process. This is probably related to presence of thin film of water between the coating and bacteria which inhibits the photocatalytic effect of the coating. Hence, only hydrophobic TiO_2/polysiloxane thin films were used in this study. Adhesion tests (in absence of UVA) conducted during 3.5 h using TiO_2/polysiloxane (results are not shown for the sake of brevity) lead to negligible decrease of bacteria concentration. Similar results (negligible decrease) were obtained for bacteria inactivation during UVA disinfection and using H_2O_2 (10 mg L^{-1}) only.

As shown in Fig. 5, the typical for photocatalytic disinfection shoulder (Fernández-Ibáñez et al., 2015) was observed during photocatalytic and H_2O_2-assisted photocatalytic disinfection. In terms of inactivation rate, according to "Log-linear + shoulder" model, disinfection was about 2.7 times higher in case of H_2O_2-assisted photocatalysis (k_{max} = 0.166 $W^{-1}h^{-1}m^2$) as compared to photocatalysis with TiO_2/polysiloxane (k_{max} = 0.063 $W^{-1}h^{-1}m^2$). Obtained results are in agreement with earlier studies (Jiménez-Tototzintle et al., 2018), where enhanced bacteria inactivation was obtained using TiO_2-immobilized/H_2O_2/UVA. Inactivation rate of UVA/H_2O_2 (initial concentration 10 mg L^{-1}) cannot be directly compared with inactivation rates obtained for photocatalysis and H_2O_2-assisted photocatalysis as results fit "Log-linear" model. However, taking into consideration UV dose required for elimination of 4 LRV of bacteria, the highest performance was achieved in case of H_2O_2-assisted photocatalysis (87.2 Wh m^{-2}, 113 min), while it was similar order of magnitude for UVA/H_2O_2 (169.8 Wh m^{-2}, 219 min) and photocatalysis (196.3 Wh m^{-2}, 253 min).

After application of photocatalysis (180 min) and H_2O_2-assisted photocatalysis (120 min), water samples were taken and stored during 24 h in dark conditions at room temperature (Table S3). Interestingly, no regrowth was observed after 24 h for water disinfected using H_2O_2-assisted photocatalysis, while opposite was true in case of photocatalysis. These results were not surprising taking into consideration following factors: *(i)* higher bacteria survival was observed immediately after photocatalysis (56 CFU mL^{-1}) as compared with H_2O_2-assisted photocatalysis (1 CFU mL^{-1}); *(ii)* presence of residual H_2O_2 in water treated by H_2O_2-assisted photocatalysis prevent bacterial regrowth due to residual H_2O_2 concentration (7.6 ± 1 mg H_2O_2 L^{-1} after 24 h). Consulting the scientific literature, bacteria regrowth after application of photocatalytic disinfection has been reported earlier (Levchuk et al., 2018), which can be possibly attributed to increase of biodegradable organic matter occurring during photocatalysis (Thayanukul et al., 2013). Moreira et al. (2018) have compared several solar-based treatment methods (H_2O_2, TiO_2-P25 and GO-TiO_2 photocatalysis, photo-Fenton) and reported absence of bacteria regrowth after 3 days storage for all H_2O_2-assisted processes, which is in agreement with our results.

It is of high importance to study possible release of titanium from photocatalyst in order to evaluate stability of tested photocatalytic material in brackish water. Hence, concentration of titanium was determined in water samples collected before (control) and after bacteria inactivation using photocatalysis and H_2O_2-assisted photocatalysis. Interestingly, concentration of dissolved titanium in all water samples was very similar (mean concentration 5.44 ± 0.8 μg L^{-1}), suggesting that no release of titanium occurred after photocatalysis and H_2O_2-assisted photocatalysis. Additional samples of tested water were taken and concentration of titanium was measured in order to confirm detected concentration of titanium. Very similar concentrations were obtained. According to the literature, concentration of titanium present in natural water varies from 0.01 to 5.5 μg L^{-1} (Skrabal, 2006; Yan et al., 1991; Yokoi & van den Berg, 1991).

3.3. Costs of UVA-based AOPs at laboratory scale

Preliminary cost estimation was performed for UVA-based AOPs technologies considering UVA dose required for reaching 4 LRV of bacteria inactivation. Electrical consumption of pumps, peripheral electric devices and maintenance were not considered in this cost evaluation, because all experiments were carried out in laboratory scale. Thus, only costs of electrical LEDs consumption and required chemicals were included in our preliminary operational cost evaluation. It should be mentioned that the cost of electrical consumption of LEDs lamps was calculated for LEDs used in this study (laboratory scale). So, one should

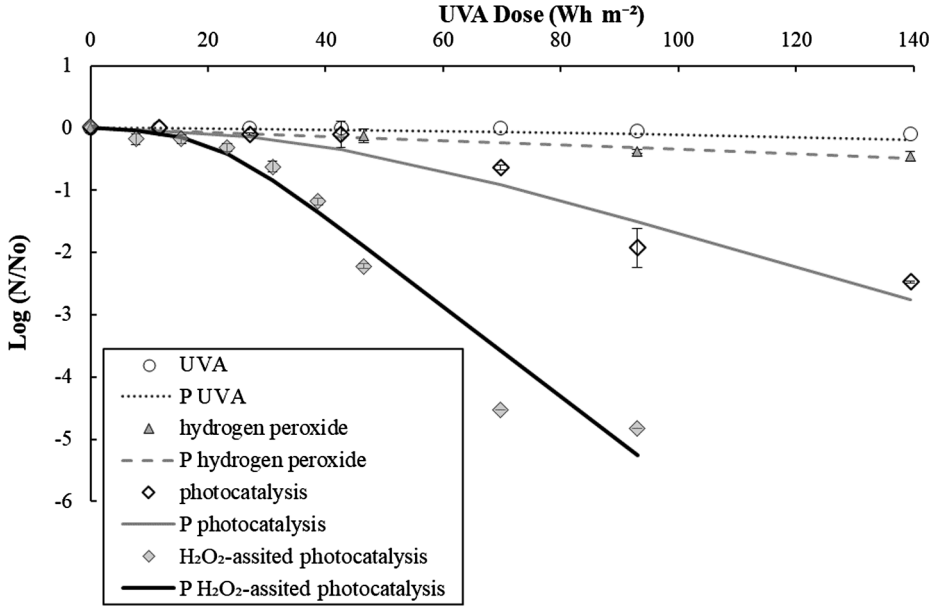

Fig. 5. Results of target bacteria inactivation in SAS by UVA-TiO_2/polysiloxane (photocatalysis), UVA-TiO_2/polysiloxane/H_2O_2 (H_2O_2-assisted photocatalysis), UVA (UVA disinfection in absence of H_2O_2) and H_2O_2 in absence of light (10 mg L^{-1}) during 3 h at room temperature (22 ± 2 °C). Symbols represents experimental data. Lines (P) represents predicted values of kinetic disinfection model.

keep in mind that such cost evaluation can be used as an indicator for comparing different disinfection technologies, while the cost of these technologies in pilot/industrial scale would be very different as the characteristics of LEDs would vary.

The electrical consumption of UVA-LEDs per volume of water (EC) was calculated using the following equation (Eq. 6) (Moreno-Andrés et al., 2020).

$$EC = \frac{I \cdot V \cdot h}{Vol} \text{ (Wh L}^{-1}\text{ or kWh m}^{-3}\text{)} \quad (6)$$

where I is electrical current (1.3 A), V is input voltage (48 V), h is exposition time (h) and Vol is illuminated volume (1.2 L).

As experiments were performed in Finland, the cost of electricity for industry in Finland was 0.067 € $kW^{-1}h^{-1}$ (BMWi Statista, 2017). The price of H_2O_2 was calculated estimated to be 0.70 € kg^{-1} (Baresel et al., 2019). Preliminary cost estimation (electrical consumption and reagents) are shown in Table 3.

The operational costs calculated for photocatalytic disinfection (14.7 € m^{-3}) was the highest in this study. It should be noticed that the estimated operational costs do not include the price of TiO_2/polysiloxane (production cost), because durability/aging of photocatalyst was not studied in this work. Therefore, the exact replacement time of TiO_2/polysiloxane is not known. However, an attempt to evaluate the price of TiO_2/polysiloxane was made. Thus, the price of TiO_2 ink preparation was estimated to be around 247 € L^{-1} (Fig. 6).

Considering the ratio of TiO_2/polysiloxane geometrical surface area to water volume, it can be estimated that about 45 m^2 of TiO_2/polysiloxane would be required for reactor able to treat 1 m^3 of water (in view of experimental procedure employing 540 cm^2 of photocatalyst to treat 1.2 L of water to reach UVA dose needed for 4 LRV inactivation of target bacteria). The cost of TiO_2/polysiloxane deposition (coating with thickness of about 250 nm) is 0.06 € m^{-2}. So, the total cost of TiO_2/polysiloxane ink jet deposition for a reactor able to treat 1 m^3 of water would be about 2.7 € (for 45 m^2). Recently, it was demonstrated that the costs for the preparation of 1L on printable TiO_2/polysiloxane ink can be reduced from 247 € L^{-1} to ~50 € L^{-1} using different TiO_2 nanoparticles (Pretiox CG100, Precheza) having similar photocatalytic effect (Homola et al., 2020). This can lead to further decrease in operation costs.

As it was mentioned above, the durability of TiO_2/polysiloxane thin films for aquaculture water stream disinfection was not studied in this work. Hence, it is difficult to estimate the cleaning/replacement time of the photocatalyst and its cost. In our earlier work (Levchuk et al., 2019), in which the same material was used for solar photocatalytic disinfection of simulated aquaculture water, the significant decrease of activity was observed after 15 h of contact time (10 photocatalytic cycles) and attributed to deposition of salts on the surface. Thus, in the worst scenario (photocatalyst replacement takes place each 15 h), the cost of photocatalyst per m^3 of treated water would be 0.8 €. In this case, the operational cost of photocatalysis (electrical cost of LEDs consumption and production cost of photocatalyst) can be estimated as 15.5 € m^{-3}.

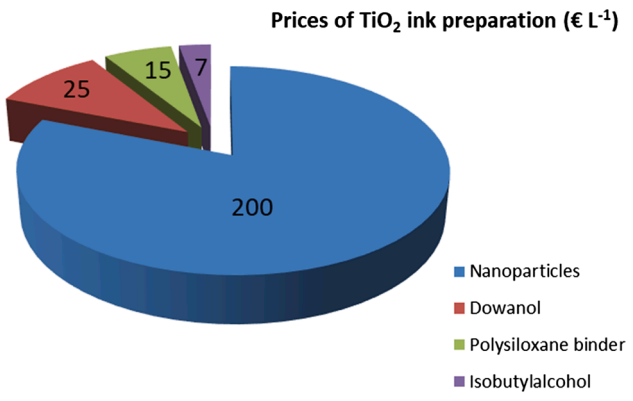

Fig. 6. Constituents of the cost for photocatalyst ink (1 L).

Addition of hydrogen peroxide (10 mg L^{-1} of H_2O_2) to the photocatalytic system (H_2O_2-assisted photocatalysis) allowed to decrease the electrical cost of LEDs consumption about two times (6.6 € m^{-3}). Taking into account that lower UVA dose was required to reach 4 LRV by H_2O_2-assisted photocatalysis in comparison with photocatalysis, the cost of photocatalyst per m^3 of treated water would be 0.6 € (photocatalyst replacement takes place each 15 h). So, the operational cost of H_2O_2-assisted photocatalysis (electrical cost of LEDs consumption and production cost of photocatalyst) could be 7.2 € m^{-3}.

The costs estimated for UVA/H_2O_2 process at optimal conditions (10 mg H_2O_2 L^{-1}, 3.65 h) was 12.7 € m^{-3}. The major contribution (>99%) to the cost of this process is electrical consumption of UVA-LEDs. According to results obtained in this work, the cost of UVA/H_2O_2 process conducted at 22 ± 1 °C can be significantly decreased if water is stored for 24 h with H_2O_2 (10 mg L^{-1}) in absence of light and only after that UVA irradiation is applied. This is a very promising option, which allows to decrease the electrical cost of UVA-LEDs almost four times (3.2 € m^{-3}), being the lowest operational cost among studied in this work UVA-based AOPs. An important factor for application of UVA/H_2O_2 disinfection is presence of residual H_2O_2 in water (in our experiments 7.7 ± 0.3 mg L^{-1}). According to the literature, a concentration of H_2O_2 between 10 and 37 mg L^{-1} was observed to be not toxic in RAS water streams (Schmidt et al., 2006).

In summary, the electrical cost of UVA-LEDs significantly contributes to the operational costs of studied UVA-based AOPs, making these processes economically not feasible. Hence, an alternative source of irradiation (natural sunlight) was studied.

3.4. Solar-based AOPs

3.4.1. Bacterial inactivation

Taking into consideration that optimal H_2O_2 concentration for UVA/H_2O_2 experiments conducted in this study was 10 mg L^{-1}, this concentration was chosen for SODIS/H_2O_2 tests in Finland. SODIS (in absence of H_2O_2) was conducted as reference test. Moreover, SODIS/H_2O_2 was performed in Spain using same H_2O_2 concentration, experimental set up and SAS prepared in the same way. The latter was done in order to compare efficiency of SODIS/H_2O_2 in different climatic zones with significant difference in solar irradiance and temperature regimes. Experimental results were fitted to ″Log-Linear + shoulder″ and ″Log-Linear + tail″ models for the experiments performed in Finland and Spain, respectively (Table S2). Results are shown in Fig. 7.

Fig. 7 shows that enhanced inactivation of target bacteria in SAS was achieved when SODIS/H_2O_2 was applied in comparison with SODIS. Thus, disinfection rate constant of SODIS/H_2O_2 was about two times higher (Table 2) than that for SODIS (experiments conducted in Finland). Bacteria regrowth after 24 h was not observed in the samples containing hydrogen peroxide. However, regrowth of 0.15% (Table S3) was observed after SODIS. Similar results were observed in *section 3.2.2*.

In order to compare efficiency of SODIS/H_2O_2 carried out in Finland and Spain, crucial parameters for SODIS/H_2O_2 were summarized in Table 2.

Significant differences were observed for such parameters of SODIS/H_2O_2 as irradiance and temperature (Table 2). Thus, mean solar irradiance and mean temperature were about three times and almost six times lower in Finland than in Spain, respectively. Experimental results revealed that the inactivation rate was significantly higher for SODIS/H_2O_2 tests performed in Finland (k_{max} = 0.589 m^2 $W^{-1}h^{-1}$, SL = 9.12 Wh m^{-2}; autumn) in comparison with ones conducted in Spain (k_{max} = 0.312 m^2 $W^{-1}h^{-1}$, N_{res} = 0.198 CFU mL^{-1}; summer). The solar radiation dose required to reach 4 LRV (D_4) was 22% lower in Finland than in Spain. However, due to the fact that irradiance was lower in Finland, the experimental time required to reach certain UV dose (e.g. for 4 LRV) was longer in Finland than in Spain. Thus, the experimental time required to reach 4 LRV was 114 and 44 min in Finland and Spain, respectively. However, after 120 min of experimental time in Finland (27 Wh m^{-2})

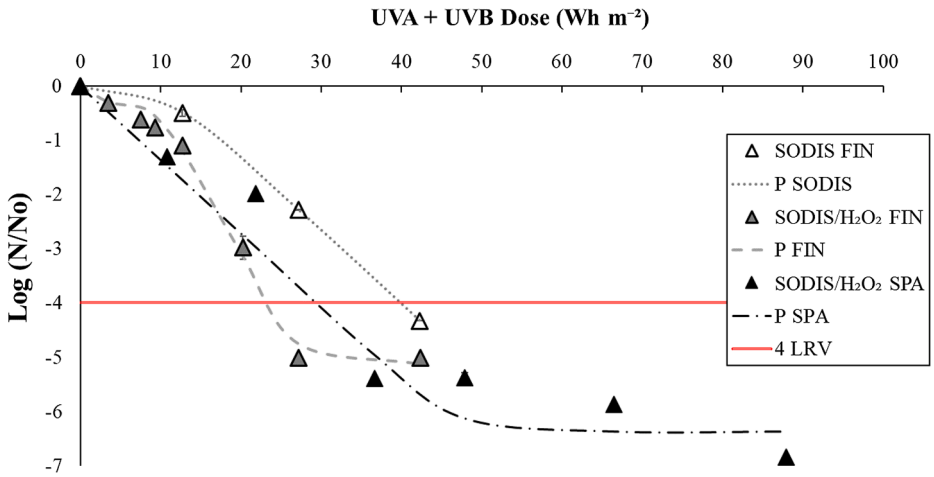

Fig. 7. Solar disinfection experiments carried out in Finland (FIN) with and without hydrogen peroxide and Spain (SPA). Symbols represents experimental data. Lines (P) represents predicted values of kinetic disinfection model.

Table 2
Experimental parameters and results of SODIS/H_2O_2 experiments conducted in Spain and Finland.

Country	Irradiation (W m^{-2})	Salinity (‰)	Water temperature (°C)	Ambient temperature (°C)	T (365 nm, %)	Fe (μg L^{-1})	TOC (mg L^{-1})	H_2O_2 (mg L^{-1})	N_i* (CFU mL^{-1})	D_4 ** (Wh m^2)	k_{max} (m^2 $W^{-1}h^{-1}$)	time D_4 (min)
Finland	13	4.9	5–7	5–7	96.0	13.7	8.2	0	$1.1{\cdot}10^5$	40	0.312	185
Finland	13	4.9	5–7	5–7	96.0	13.7	8.2	10	$1.0{\cdot}10^5$	25	0.589	114
Spain	44	35.0	31–32	33–35	96.4	9.5	1.1	10	$2.2{\cdot}10^6$	32	0.312	44

* N_i is initial bacteria concentration.
**D_4 is UV dose required to achieve 4 LRV.

the concentration of bacteria reached 0 CFU mL^{-1}, which did not occur in Spain after the same time (120 min, 88 Wh m^{-2}). Obtained results are particularly intriguing as experiments were conducted under "unfavorable" conditions in Finland and favorable conditions in Spain.

These differences can be possibly attributed to the nature of the water and the temperature of water during SODIS/H_2O_2 experiments. The hypothesis to be tested under controlled conditions is whether a lower lethal dose is needed at low temperatures. To the best of our knowledge positive effect, i.e. increase in the rate of inactivation and decrease in the lethal dose of solar radiation, of lower temperatures than 15–20 °C on efficiency of SODIS or SODIS/H_2O_2 were not reported (Giannakis et al., 2015; Vivar et al., 2017). Hence, it was decided to study the effect of low water temperature (6 °C) in available controlled conditions using UVA as irradiation source in order to understand possible effect of such temperature on inactivation efficiency using UVA-based AOPs.

3.4.2. *Cost estimation of solar-based AOPs*

Preliminary operation and maintenance (O&M) costs of SAS water disinfection (4 LRV of bacteria inactivation) were estimated in this work. Calculations were performed for raceway reactor (pilot scale) with flow 100 m^3 h^{-1} operating 365 days per year (24 h). The consumption of H_2O_2 and maintenance of raceway were included to the preliminary O&M cost estimation for solar-based AOPs. Electrical costs of pumps were not included for O&M cost estimation for solar-based AOPs. This is due to the fact that raceway reactor was designed with slight inclination, leading to water circulation through the reactor with desired speed without need of pumping. In respect of estimation was performed for 24 h operation, during the absence of solar light, conventional UVC disinfection was included. Electrical consumption of pumps, UVC lamps and maintenance of the equipment were considered in case of UVC disinfection operating during absence of solar light. The O&M simulation was conducted for two different scenarios, namely, *(i)* for reactor operated in South of Spain (Cádiz) and *(ii)* for reactor operated in the South of Finland (Helsinki). The surface area required for construction of raceway reactor in Spain was estimated to be 1700 m^2 (Rivera-Torres, 2017). However, taking into account that mean solar irradiance in South of Finland is about two times lower than that in South of Spain, the surface area required for construction of raceway reactor in Finland would be two times higher (two reactors of 1700 m^2 each). Moreover, investment cost of raceway reactor in Finland can be considered to be higher than in Spain due to greenhouse installation and its maintenance (was not considered in this estimation). Detailed design of considered raceway reactor is described elsewhere (Rivera-Torres, 2017). Detailed description of parameters taken into consideration for preliminary O&M cost evaluation can be found in our previous work (Villar-Navarro et al., 2019) . Detailed results with calculations are shown in Tables S4 and S5.

Despite the difference of mean annual number of hours suitable for solar disinfection, electricity cost, labor costs in Finland and Spain (Tables S4 and S5), the estimated O&M cost of SAS water disinfection using solar-based AOPs in combination with UVC was very similar (0.042 € m^{-3} in Spain and 0.043 € m^{-3} in Finland). Based on preliminary cost evaluation, it can be suggested that solar-based AOPs (SODIS/H_2O_2) are more economically feasible option than UVA-based AOPs (UVA/H_2O_2, photocatalysis, H_2O_2-assisted photocatalysis).

Despite the fact that cost of SAS disinfection using solar-based AOPs is relatively low it is still about two times higher than conventional UVC disinfection (~0.022 € m^{-3}) due to the maintenance costs associated with a larger infrastructure. However, carbon footprint generated during UVC disinfection (in case of continuous operation during whole year) was estimated to be ~ 6070 $kgCO_2e$ $year^{-1}$ in Finland and ~ 10741 $kgCO_2e$ $year^{-1}$ in Spain (considering 0.1362 $kgCO_2e$/kWh for Finland (Carbon Footprint Ltd, 2020) and 0.241 $kgCO_2e$/kWh for Spain (Oficina Catalana del Canvi Climàtic, 2020)). An attempt to estimate number of trees needed to capture amount of CO_2 emitted during

disinfection process per year was made taking into consideration that *Pinus sylvestris* (9.97 kg CO_2/year per tree (Ezquiaga Domínguez, 2010)) and *Pinus pinea* (13.51 kg CO_2/year per tree (Ezquiaga Domínguez, 2010)) are among most common trees in south of Finland and south of Spain, respectively. Thus, in case of continuous UVC disinfection only (whole year) ~ 608 trees (*Pinus sylvestris*) and ~ 795 trees (*Pinus pinea*) would be required to capture emitted during whole year CO_2. Application of solar-based AOPs (SODIS/H_2O_2) during available hours of sunlight in combination of UVC disinfection decrease the carbon footprint in Finland by 20.6% reaching the value of ~ 4821 $kgCO_2e$ $year^{-1}$ (corresponding to ~ 483 trees of *Pinus sylvestris*) and in Spain by 35% reaching the value of ~ 6988 $kgCO_2e$ $year^{-1}$ (corresponding to ~ 517 trees of *Pinus pinea*).

3.5. Effect of low water temperature (6 °C) on inactivation of target bacteria during UVA-based AOPs

The experiments at controlled ambient and water temperature of 6 ± 1 °C were conducted for H_2O_2-assisted UVA disinfection (UVA/H_2O_2), photocatalysis (UVA-TiO_2/polysiloxane) and H_2O_2-assisted photocatalysis. In all cases, the concentration of H_2O_2 (when added) was 10 mg L^{-1}. Results are shown in Fig. 8.

As shown in Table 3, the inactivation rate during UVA/H_2O_2 process was significantly higher when the experiment was performed at low water temperature (6 ± 1 °C) in comparison with those conducted at room temperature (22 ± 1 °C). More specifically, at low water temperature conditions the inactivation rate (k_{max} = 0.296 m^2 Wh^{-1}; SL = 20.30 Wh m^{-2}; R^2 = 0.935) was five times more this value obtained at room water temperature (k_{max} = 0.057 m^2 Wh^{-1}; R^2 = 0.982). The irradiation dose required to achieve 4 LRV was about 3.3 times lower when ambient temperature was 6 ± 1 °C in comparison with that of 22 ± 1 °C (Table S2). In both cases, as shown in Table S3, there was no regrowth of bacteria due to the presence of residual hydrogen peroxide.

Results (Fig. 8) revealed that for each of the two processes, photocatalysis and H_2O_2-assisted photocatalysis, better results were observed at 6 °C than at 22 °C. The inactivation rate of photocatalytic test conducted at 6 ± 1 °C (k_{max} = 0.080 m^2 Wh^{-1}; SL = 25.6 Wh m^{-2}; R^2 = 0.943) was 1.3 times higher in comparison with that at 22 ± 1 °C (k_{max} = 0.063 m^2 Wh^{-1}; SL = 38.3 Wh m^{-2}; R^2 = 0.941) with irradiation dose required for 4 LRV of 145.7 Wh m^{-2} and 196.3 Wh m^{-2}, respectively. Inactivation rate of H_2O_2-assisted photocatalysis at low temperature (k_{max} = 0.182 m^2 Wh^{-1}; SL = 19.7 Wh m^{-2}; R^2 = 0.904) was 1.1 times higher than at room temperature (k_{max} = 0.166 m^2 Wh^{-1}; SL = 20.2 Wh m^{-2}; R^2 = 0.970) with the irradiation dose needed for 4 LRV of 75.6 Wh m^{-2} (6 ± 1 °C) and 87.2 Wh m^{-2} (22 ± 1 °C), respectively. The summary of results regarding the kinetics of bacterial inactivation of all disinfection treatments at 22 °C and 6 °C can be found in Table S2.

Observed in this study results can be explained by the fact that at lower studied water temperatures (6 ± 1 °C) the bacterial metabolism slow down significantly, so that the capacity for cell regeneration and repair is lower. In such conditions, effect of UVA and solar-based AOPs studied disinfection methods on bacteria inactivation is significantly higher. Suggested mechanism is in agreement with previous studies (Jiravanichpaisal et al., 2009; Korkut et al., 2018) in which a much lower growth rate of *Aeromonas hydrophila* and *Pseudomonas gessardi* has been observed at 6 °C in comparison with 22 °C. In the study of Jiravanichpaisal et al., (2009) a low mortality of crayfish in the presence of *A. hydrophila* at low temperatures (4°) was related to the fact that the bacteria do not replicate or their replication is very low.

Effect of H_2O_2 addition to photocatalytic process on regrowth was observed (Table S3). In the case of H_2O_2-assisted photocatalysis conducted at 6 ± 1 °C and 22 ± 1 °C no regrowth (24 h) was observed, while it was observed for photocatalysis. Thus, regrowth of bacteria was about 0.5% in SAS treated by photocatalysis at low temperature and stored during 24 h. It should be mentioned that possibly due to higher efficiency of bacteria inactivation by low temperature photocatalysis (6 ± 1 °C), the regrowth was significantly lower (0.5%) in comparison with that for photocatalysis conducted at room temperature (5.41%) (temperature of storage was 22 ± 1 °C for both cases). Therefore, the addition of hydrogen peroxide to photocatalytic system not only increases the rate of disinfection but also prevent bacteria regrowth.

Table 3 also shows cost estimation of UVA-based AOPs performance at 22 °C (discussed in *section 3.3*) and 6 °C. It should be mentioned that when UVA/H_2O_2 is conducted at low temperature (6 ± 1 °C), the dose required for 4 LRV significantly decrease, which, in turn, leads to decrease of operational costs>70% (3.8 € m^{-3}). The efficiency of

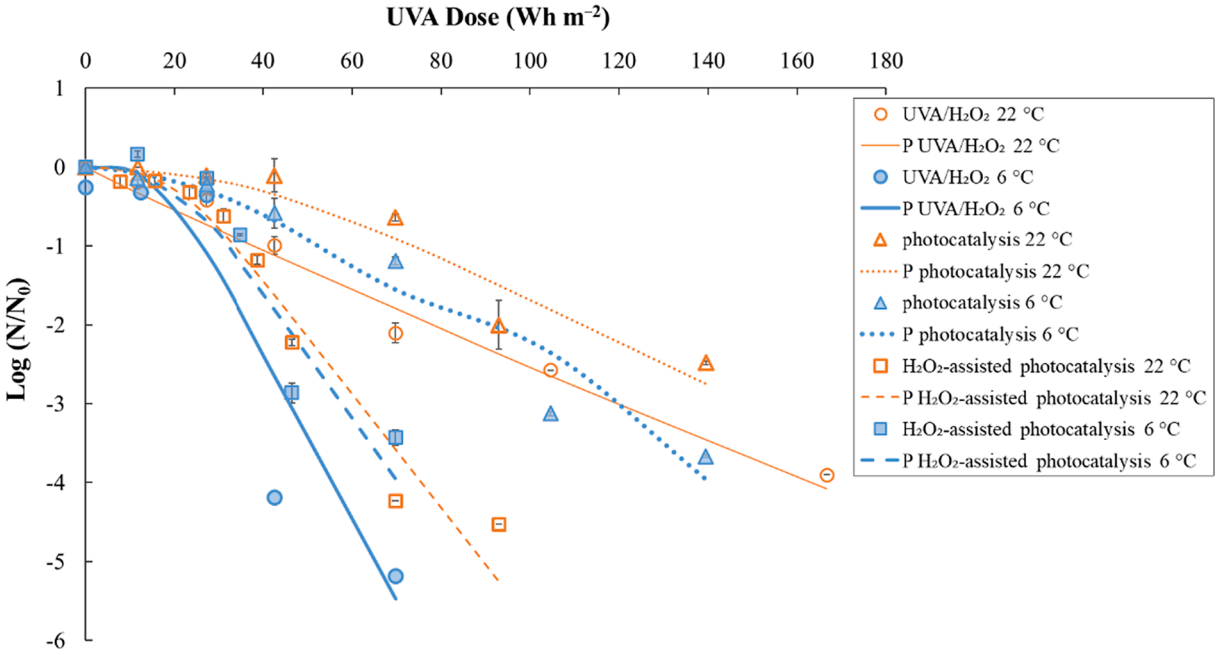

Fig. 8. Bacterial inactivation of target bacteria in SAS water using: UVA/H_2O_2 disinfection, UVA-TiO_2/polysiloxane (photocatalysis), UVA-TiO_2/polysiloxane-H_2O_2 (H_2O_2-assisted photocatalysis) at low temperature (6 ± 1 °C) and at room temperature (22 ± 1 °C). Symbols represents experimental data. Lines (P) represents predicted values of kinetic disinfection model.

Table 3
Disinfection kinetics of the studied treatment methods. Dose for 4 Log Removal Value (D_4), maximum specific inactivation rate (k_{max}), shoulder length (SL), determination coefficient (R^2) and preliminary cost estimation of different disinfection technologies, being TC_4 operational cost for 4 LRV. D_4 was calculated according to k_{max} value obtained for each treatment. The concentration of hydrogen peroxide, in all cases, was 10 mg L^{-1}. The ″Log-Linear + shoulder″ model was used in all cases except the first one (Log-Linear).

Experiment	D_4; Wh m^{-2} (min)	$k_{max} \pm$ S.E.; m^2 $W^{-1}h^{-1}$	SL ± S.E.; Wh m^{-2}	R^2	Electrical consumption (kWh m^{-3})	Reagent cost (€ cent m^{-3})	TC_4 (€ m^{-3})
UVA/H_2O_2 22 °C	169.8 (219)	0.057 ± 0.005	–	0.982	190	0.7	12.7
UVA/H_2O_2 6 °C	50.9 (66)	0.296 ± 0.092	20.30 ± 11.21	0.935	57.2	0.7	3.8
Photocatalysis 22 °C	196.3 (253)*	0.063 ± 0.013	38.25 ± 18.97	0.941	217.5	–	14.6
Photocatalysis 6 °C	145.7 (188)	0.080 ± 0.015	25.55 ± 19.28	0.943	165.5	–	10.9
H_2O_2-assisted photocatalysis 22 °C	87.2 (113)	0.166 ± 0.016	20.17 ± 6.19	0.970	100.5	0.7	6.6
H_2O_2-assisted photocatalysis 6 °C	75.6 (97)	0.182 ± 0.049	19.68 ± 11.76	0.904	84	0.7	5.6

*Predicted value with dose not reached during experimentation.

photocatalysis and H_2O_2-assisted photocatalysis conducted at low water temperature (6 ± 1 °C) was also higher, which led to decrease of electrical costs associated to UVA-LEDs (the major contribution of the operational cost). Thus, the total costs to achieve 4 LRV (TC_4) were reduced by a 17 and 23% for UVA TiO_2/polysiloxane/H_2O_2 and UVA TiO_2/polysiloxane disinfection, respectively.

4. Conclusions

In this study, two irradiation sources, UVA-LEDs and natural solar light, were tested for disinfection of SASs with wild bacteria. The effect of low temperature on the lethal irradiation dose and operational treatment costs were analysed. The main relevant outcomes are outlined below.

- Bacterial inactivation was not observed using UVA disinfection in the absence of hydrogen peroxide. After 180 min of exposure (140 Wh m^{-2}) inactivation reached 19%. Bacteria inactivation increases with rise of initial hydrogen peroxide concentration in absence of light within an interval 5 – 24 h (contact time). Bacterial inactivation does not occur after 24 h storage when H_2O_2 concentrations are above 2.5 mg L^{-1}.
- UVA dose required for 4 LRV decreased from 382.9 to 145.3 Wh m^{-2} when between 5 and 15 mg of H_2O_2 L^{-1} was used. No significant bacterial reduction was observed during use of concentrations below 2.5 mg L^{-1} when 140 Wh m^{-2} was applied. The concentration 10 H_2O_2 mg L^{-1} was taken as the optimal concentration. The dose needed to reach 4 LRV decreased more than three times at low temperature (6 ± 1 °C) from 145.3 to 50.9 Wh m^{-2}. No regrowth was observed after 24 h in samples where hydrogen peroxide was present during the experiment. It was observed that a 24-hour exposure to hydrogen peroxide (10 mg L^{-1}) prior to UVA irradiation can reduce the dose needed to reach 4 LRV by almost four times at room temperature (22 ± 1 °C). The costs of UVA/H_2O_2 treatment at optimal concentration (10 mg L^{-1}) reached 12.7 € m^{-3}. Improvements were found if the experiment was performed at low temperature or if there was previous exposure (24 h) to hydrogen peroxide, dropping the cost to 3.8 and 3.2 € m^{-3}, respectively.
- H_2O_2-assisted photocatalysis enhance bacterial inactivation (k_{max}) by 62% compared to photocatalysis at 22 ± 1 °C. More specifically, the required dose for 4 LRV reduced from 196.3 to 87.2 Wh m^{-2} if hydrogen peroxide was added. Low temperature (6 ± 1 °C) affected the kinetic inactivation rate significantly but to a lesser extent than with UVA/H_2O_2 reaching doses for 4 LRV of 145.7 and 75.6 Wh m^{-2} for photocatalysis and H_2O_2-assisted photocatalysis process, respectively. There was no regrowth at low temperature or room temperature if hydrogen peroxide was added. In absence of hydrogen peroxide the percentage of regrowth was lower in experiments carried out at low temperature (0.49 %) than at room temperature (>5 %) while samples were preserved at room temperature. Although cleaning and replacement costs were not estimated, the electrical costs of H_2O_2-assisted photocatalysis and photocatalysis at 22 °C were 14.6 and 6.6 € m^{-3}. The effect of low temperature affected the cost of the treatment, reducing them by 15% for H_2O_2-assisted photocatalysis and 25% for photocatalysis process.
- The performance of SODIS treatment in areas with low irradiance as in the Nordic countries is comparable to that of other areas with higher irradiance due to the effect of low temperatures (6 ± 1 °C). As observed in other treatments, the addition of hydrogen peroxide prevented bacterial regrowth. In the case of the absence of hydrogen peroxide, a regrowth of 0.15% occurred after 24 h when samples were preserved at room temperature. The costs for SODIS/H_2O_2 in Spain and Finland were very similar: 0.042 € m^{-3} in Spain and 0.043 € m^{-3}. Furthermore, the use of SODIS combined with UVC reduces the carbon footprint by 20.6% in Finland and 35% in Spain compared to the continued use of traditional UVC treatment.
- A synergistic effect of low temperatures has been observed in treatments with SODIS, UVA/H_2O_2, UVA/TiO_2/polysiloxane and UVA/TiO_2/polysiloxane/H_2O_2, increasing inactivation kinetics (k_{max}) between 1.1 and 5.2 times.
- It has been proposed that the effect of low temperature on the inactivation of bacteria is based on the reduction of cell metabolism that slows down the replication and repair rate of bacteria.

Future work will have to determine more specifically the molecular mechanisms by which organisms are particularly affected during low temperature disinfection by solar and UVA irradiation and the joint effect with the addition of hydrogen peroxide. In addition, it will be essential to carry out experiments with real aquaculture water samples to verify that the resistance of the bacteria is similar to those studied here.

Declaration of Competing Interest

The authors declare that they have no known competing financial interests or personal relationships that could have appeared to influence the work reported in this paper.

Acknowledgements

This work was supported by a national research project (SUNRAS PROJECT, Project AGL2016-80507-R) funded by Ministerio de Economía y Competitividad (Plan Nacional de I + D + i (2013-2016). The research was also supported by a PIF contract (UCA/REC01VI/2017) funded by Vicerrectorado de Investigación of Universidad de Cádiz. D. Sc. Juan Jose Rueda-Marquez is grateful for financial support from Academy of Finland within the project ″Combination of Advanced Oxidation Processes and Photobiotreatment for Sustainable Resource

Recovery and Wastewater Reuse″ (application number 322339). T. Homola acknowledges financial support by Czech Science Foundation project 19-14770Y and project LM2018097 funded by the Ministry of Education, Youth and Sports of the Czech Republic.

Appendix A. Supplementary data

Supplementary data to this article can be found online at https://doi.org/10.1016/j.solener.2021.09.029.

References

APHA/WEF/AWWA. (2018a). 9222 Membrane filter technique for members of the coliform group (2017). In Standard Methods For the Examination of Water and Wastewater. American Public Health Association. https://doi.org/doi:10.2105/SMWW.2882.193.

APHA/WEF/AWWA. (2018b). Standard Methods For The Examination of Water and Wastewater (23rd ed.). Washington, DC, New York.

Badiola, M., Basurko, O.C., Piedrahita, R., Hundley, P., Mendiola, D., 2018. Energy use in Recirculating Aquaculture Systems (RAS): A review. Aquacult. Eng. 81, 57–70. https://doi.org/10.1016/J.AQUAENG.2018.03.003.

Baresel, C., Harding, M., Junestedt, C., 2019. Removal of pharmaceutical residues from municipal wastewater using UV/H2O2. *IVL Swedish Environmental Research Institute, Rep.* B2354 (September).

Ben-Asher, R., Ravid, S., Ucko, M., Smirnov, M., Lahav, O., 2019. Chlorine-based disinfection for controlling horizontal transmission of VNN in a seawater recirculating aquaculture system growing European seabass. Aquaculture 510, 329–336. https://doi.org/10.1016/J.AQUACULTURE.2019.06.001.

BMWi Statista. (2017). Prices of electricity for industry in Finland from 1995 to 2017. Retrieved May 10, 2020, from https://www.statista.com/statistics/595853/electricity-industry-price-finland/.

Carbon Footprint Ltd. (2020). Carbon Footprint Calculator For Individuals and Households. Retrieved September 14, 2020, from https://www.carbonfootprint.com/calculator.aspx.

Chang, M.H., Das, D., Varde, P.V., Pecht, M., 2012. Light emitting diodes reliability review. Microelectron. Reliab. 52 (5), 762–782. https://doi.org/10.1016/j.microrel.2011.07.063.

Chhetri, R.K., Baun, A., Andersen, H.R., 2019. Acute toxicity and risk evaluation of the CSO disinfectants performic acid, peracetic acid, chlorine dioxide and their by-products hydrogen peroxide and chlorite. Sci. Total Environ. 677, 1–8. https://doi.org/10.1016/J.SCITOTENV.2019.04.350.

Culot, A., Grosset, N., Gautier, M., 2019. Overcoming the challenges of phage therapy for industrial aquaculture: A review. Aquaculture 513, 734423. https://doi.org/10.1016/j.aquaculture.2019.734423.

Dauda, A.B., Ajadi, A., Tola-Fabunmi, A.S., Akinwole, A.O., 2019. Waste production in aquaculture: Sources, components and managements in different culture systems. Aquaculture and Fisheries 4 (3), 81–88. https://doi.org/10.1016/J.AAF.2018.10.002.

Davidson, J., Good, C., Welsh, C., Summerfelt, S., 2011. The effects of ozone and water exchange rates on water quality and rainbow trout Oncorhynchus mykiss performance in replicated water recirculating systems. Aquacult. Eng. 44 (3), 80–96. https://doi.org/10.1016/J.AQUAENG.2011.04.001.

Edwards, P., 2015. Aquaculture environment interactions: Past, present and likely future trends. Aquaculture 447, 2–14. https://doi.org/10.1016/j.aquaculture.2015.02.001.

Ezquiaga Domínguez, J.M., 2010. Estrategias de adaptación y mitigación del Cambio Climático en planificación espacial. Gobierno Vasco.

FAO. (2018). The State of World Fisheries and Aquaculture 2018 - Meeting the sustainable development goals. Fao. Retrieved from http://www.fao.org/state-of-fisheries-aquaculture.

Feng, Ling, Peillex-Delphe, Céline, Lü, Changwei, Wang, Da, Giannakis, Stefanos, Pulgarin, Cesar, 2020. Employing bacterial mutations for the elucidation of photo-Fenton disinfection: Focus on the intracellular and extracellular inactivation mechanisms induced by UVA and H2O2. Water Res. 182, 116049. https://doi.org/10.1016/j.watres.2020.116049.

Fernández-Ibáñez, P., Polo-López, M.I., Malato, S., Wadhwa, S., Hamilton, J.W.J., Dunlop, P.S.M., D'Sa, R., Magee, E., O'Shea, K., Dionysiou, D.D., Byrne, J.A., 2015. Solar photocatalytic disinfection of water using titanium dioxide graphene composites. Chem. Eng. J. 261, 36–44. https://doi.org/10.1016/j.cej.2014.06.089.

Figueredo-Fernández, M., Gutiérrez-Alfaro, S., Acevedo-Merino, A., Manzano, M.A., 2017. Estimating lethal dose of solar radiation for enterococcus inactivation through radiation reaching the water layer. Application to Solar Water Disinfection (SODIS). Sol. Energy 158, 303–310. https://doi.org/10.1016/J.SOLENER.2017.09.006.

Gao, Feng, Li, Chen, Yang, Zhao-Hui, Zeng, Guang-Ming, Feng, Li-Juan, Liu, Jun-zhi, Liu, Mei, Cai, Hui-wen, 2016. Continuous microalgae cultivation in aquaculture wastewater by a membrane photobioreactor for biomass production and nutrients removal. Ecol. Eng. 92, 55–61. https://doi.org/10.1016/j.ecoleng.2016.03.046.

Geeraerd, A.H., Valdramidis, V.P., Van Impe, J.F., 2005. GInaFiT, a freeware tool to assess non-log-linear microbial survivor curves. Int. J. Food Microbiol. 102 (1), 95–105. https://doi.org/10.1016/j.ijfoodmicro.2004.11.038.

Giannakis, S., Darakas, E., Escalas-Cañellas, A., Pulgarin, C., 2014. The antagonistic and synergistic effects of temperature during solar disinfection of synthetic secondary effluent. J. Photochem. Photobiol., A 280, 14–26. https://doi.org/10.1016/j.jphotochem.2014.02.003.

Giannakis, S., Darakas, E., Escalas-Cañellas, A., Pulgarin, C., 2015. Temperature-dependent change of light dose effects on E. coli inactivation during simulated solar treatment of secondary effluent. Chem. Eng. Sci. 126, 483–487. https://doi.org/10.1016/j.ces.2014.12.045.

Giannakis, S., López, M.I.P., Spuhler, D., Pérez, J.A.S., Ibáñez, P.F., Pulgarin, C., 2016. Solar disinfection is an augmentable, in situ-generated photo-Fenton reaction—Part 2: A review of the applications for drinking water and wastewater disinfection. Appl. Catal. B 198, 431–446. https://doi.org/10.1016/J.APCATB.2016.06.007.

Gonçalves Pessoa, R.B., de Oliveira, W.F., Marques, D.S.C., dos Santos Correia, M.T., de Carvalho, E.V.M.M., Coelho, L.C.B.B., 2019. The genus Aeromonas: A general approach. Microb. Pathog. 130 (March), 81–94. https://doi.org/10.1016/j.micpath.2019.02.036.

Hamamoto, A., Mori, M., Takahashi, A., Nakano, M., Wakikawa, N., Akutagawa, M., … Kinouchi, Y. (2007). New water disinfection system using UVA light-emitting diodes. Journal of Applied Microbiology, 103(6), 2291–2298. https://doi.org/10.1111/j.1365-2672.2007.03464.x.

Homola, T., Ďurašová, Z., Shekargoftar, M., Souček, P., Dzik, P., 2020a. Optimization of TiO2 Mesoporous Photoanodes Prepared by Inkjet Printing and Low-Temperature Plasma Processing. Plasma Chem. Plasma Process. 40 (5), 1311–1330. https://doi.org/10.1007/s11090-020-10086-y.

Homola, Tomáš, Dzik, Petr, Veselý, Michal, Kelar, Jakub, Černák, Mirko, Weiter, Martin, 2016. Fast and Low-Temperature (70 °c) Mineralization of Inkjet Printed Mesoporous TiO2 Photoanodes Using Ambient Air Plasma. ACS Appl. Mater. Interfaces 8 (49), 33562–33571. https://doi.org/10.1021/acsami.6b0955610.1021/acsami.6b09556.s001.

Homola, Tomáš, Pospisil, Jan, Shekargoftar, Masoud, Svoboda, Tomáš, Hvojnik, Matej, Gemeiner, Pavol, Weiter, Martin, Dzik, Petr, 2020b. Perovskite Solar Cells with Low-Cost TiO2Mesoporous Photoanodes Prepared by Rapid Low-Temperature (70 °c) Plasma Processing. ACS Applied Energy Materials 3 (12), 12009–12018. https://doi.org/10.1021/acsaem.0c0214410.1021/acsaem.0c02144.s001.

Jiang, X., Manawan, M., Feng, T., Qian, R., Zhao, T., Zhou, G., … Pan, J. H. (2018). Anatase and rutile in evonik aeroxide P25: Heterojunctioned or individual nanoparticles? Catalysis Today, 300(December 2016), 12–17. https://doi.org/10.1016/j.cattod.2017.06.010.

Jiménez-Tototzintle, M., Ferreira, I.J., da Silva Duque, S., Guimarães Barrocas, P.R., Saggioro, E.M., 2018. Removal of contaminants of emerging concern (CECs) and antibiotic resistant bacteria in urban wastewater using UVA/TiO2/H2O2 photocatalysis. Chemosphere 210, 449–457. https://doi.org/10.1016/J.CHEMOSPHERE.2018.07.036.

Jiravanichpaisal, P., Roos, S., Edsman, L., Liu, H., Söderhäll, K., 2009. A highly virulent pathogen, Aeromonas hydrophila, from the freshwater crayfish Pacifastacus leniusculus. J. Invertebr. Pathol. 101 (1), 56–66. https://doi.org/10.1016/J.JIP.2009.02.002.

Jorquera, M.A., Valencia, G., Eguchi, M., Katayose, M., Riquelme, C., 2002. Disinfection of seawater for hatchery aquaculture systems using electrolytic water treatment. Aquaculture 207 (3–4), 213–224. https://doi.org/10.1016/S0044-8486(01)00766-9.

Joyce, T.M., McGuigan, K.G., Elmore-Meegan, M., Conroy, R.M., 1996. Inactivation of fecal bacteria in drinking water by solar heating. Appl. Environ. Microbiol. 62 (2), 399–402. https://doi.org/10.1128/aem.62.2.399-402.1996.

Kasai, H., Yoshimizu, M., Ezura, Y., 2002. Disinfection of Water for Aquaculture. Fish. Sci. 68 (sup1), 821–824. https://doi.org/10.2331/fishsci.68.sup1_821.

Korkut, G.G., Söderhäll, I., Söderhäll, K., Noonin, C., 2018. The effect of temperature on bacteria-host interactions in the freshwater crayfish, Pacifastacus leniusculus. J. Invertebr. Pathol. 157, 67–73. https://doi.org/10.1016/J.JIP.2018.08.001.

Labas, M.D., Zalazar, C.S., Brandi, R.J., Cassano, A.E., 2008. Reaction kinetics of bacteria disinfection employing hydrogen peroxide. Biochem. Eng. J. 38 (1), 78–87. https://doi.org/10.1016/j.bej.2007.06.008.

Levchuk, Irina, Homola, Tomáš, Moreno-Andrés, Javier, Rueda-Márquez, Juan José, Dzik, Petr, Moríñigo, Miguel Ángel, Sillanpää, Mika, Manzano, Manuel A., Vahala, Riku, 2019. Solar photocatalytic disinfection using ink-jet printed composite TiO2/SiO2 thin films on flexible substrate: Applicability to drinking and marine water. Sol. Energy 191, 518–529. https://doi.org/10.1016/j.solener.2019.09.038.

Levchuk, Irina, Kralova, Marcela, Rueda-Márquez, Juan José, Moreno-Andrés, Javier, Gutiérrez-Alfaro, Sergio, Dzik, Petr, Parola, Stephane, Sillanpää, Mika, Vahala, Riku, Manzano, Manuel A., 2018. Antimicrobial activity of printed composite TiO2/SiO2 and TiO2/SiO2/Au thin films under UVA-LED and natural solar radiation. Appl. Catal. B 239, 609–618. https://doi.org/10.1016/j.apcatb.2018.08.051.

Lindenauer, K.G., Darby, J.L., 1994. Ultraviolet disinfection of wastewater: Effect of dose on subsequent photoreactivation. Water Res. 28 (4), 805–817. https://doi.org/10.1016/0043-1354(94)90087-6.

Liu, D., Behrens, S., Pedersen, L.-F., Straus, D.L., Meinelt, T., 2016. Peracetic acid is a suitable disinfectant for recirculating fish-microalgae integrated multi-trophic aquaculture systems. Aquacult. Rep. 4, 136–142. https://doi.org/10.1016/J.AQREP.2016.09.002.

Ma, Dongwei, Li, Kaiming, Pan, Jia Hong, 2020. Ultraviolet-Induced Interfacial Crystallization of Uniform Nanoporous Biphasic TiO2 Spheres for Durable Lithium-Ion Battery. ACS Applied Energy Materials 3 (5), 4186–4192. https://doi.org/10.1021/acsaem.0c0081610.1021/acsaem.0c00816.s001.

Masschelein, W., Denis, M., Ledent, R., 1977. Spectrophotometric determination of residual hydrogen peroxide. Water Sewage Works 124.

Matthijs, Hans C.P., Visser, Petra M., Reeze, Bart, Meeuse, Jeroen, Slot, Pieter C., Wijn, Geert, Talens, Renée, Huisman, Jef, 2012. Selective suppression of harmful

cyanobacteria in an entire lake with hydrogen peroxide. Water Res. 46 (5), 1460–1472. https://doi.org/10.1016/j.watres.2011.11.016.
McGuigan, K.G., Joyce, T.M., Conroy, R.M., Gillespie, J.B., Elmore-Meegan, M., 1998. Solar disinfection of drinking water contained in transparent plastic bottles: Characterizing the bacterial inactivation process. J. Appl. Microbiol. 84 (6), 1138–1148. https://doi.org/10.1046/j.1365-2672.1998.00455.x.
Moreira, Nuno F.F., Narciso-da-Rocha, Carlos, Polo-López, M. Inmaculada, Pastrana-Martínez, Luisa M., Faria, Joaquim L., Manaia, Célia M., Fernández-Ibáñez, Pilar, Nunes, Olga C., Silva, Adrián M.T., 2018. Solar treatment (H2O2, TiO2-P25 and GO-TiO2 photocatalysis, photo-Fenton) of organic micropollutants, human pathogen indicators, antibiotic resistant bacteria and related genes in urban wastewater. Water Res. 135, 195–206. https://doi.org/10.1016/j.watres.2018.01.064.
Moreno-Andrés, Javier, Rueda-Márquez, Juan José, Homola, Tomáš, Vielma, Jouni, Moríñigo, Miguel Ángel, Mikola, Anna, Sillanpää, Mika, Acevedo-Merino, Asunción, Nebot, Enrique, Levchuk, Irina, 2020. A comparison of photolytic, photochemical and photocatalytic processes for disinfection of recirculation aquaculture systems (RAS) streams. Water Res. 181, 115928. https://doi.org/10.1016/j.watres.2020.115928.
Oficina Catalana del Canvi Climàtic. (2020). Factor de emisión de la energía eléctrica: el mix. Retrieved October 5, 2020, from https://canviclimatic.gencat.cat/es/actua/factors_demissio_associats_a_lenergia/.
de la Pena, L.D., Lavilla-Pitogo, C.R., Paner, M.G., 2001. Luminescent Vibrios Associated with Mortality in Pond-Cultured Shrimp Penaeus monodon in the Philippines : Species Composition. Fish Pathology 36 (3), 133–138. https://doi.org/10.3147/jsfp.36.133.
Prasad, Amritha, Du, Lihui, Zubair, Muhammad, Subedi, Samir, Ullah, Aman, Roopesh, M.S., 2020. Applications of Light-Emitting Diodes (LEDs) in Food Processing and Water Treatment. Food Eng. Rev. 12 (3), 268–289. https://doi.org/10.1007/s12393-020-09221-4.
Qi, W., Zhu, S., Shitu, A., Ye, Z., Liu, D., 2020. Low concentration peroxymonosulfate and UVA-LED combination for E. coli inactivation and wastewater disinfection from recirculating aquaculture systems. *Journal of Water*. Process Engineering 36 (May), 101362. https://doi.org/10.1016/j.jwpe.2020.101362.
Ranjan, R., Megarajan, S., Xavier, B., Raju, S.S., Ghosh, S., Gopalakrishnan, A., 2019. Design and performance of recirculating aquaculture system for marine finfish broodstock development. Aquacult. Eng. 85, 90–97. https://doi.org/10.1016/J.AQUAENG.2019.03.002.
Rincón, A.G., Pulgarin, C., 2006. Comparative evaluation of Fe3+ and TiO2 photoassisted processes in solar photocatalytic disinfection of water. Appl. Catal. B 63 (3–4), 222–231. https://doi.org/10.1016/j.apcatb.2005.10.009.
Rivera-Torres, J.M., 2017. Desinfección solar de efluentes de la acuicultura para la reutilización del agua. University of Cadiz.
Samuilov, V.D., Bezryadnov, D.V., Gusev, M.V., Kitashov, A.V., Fedorenko, T.A., 1999. Hydrogen peroxide inhibits the growth of cyanobacteria. Biochemistry 64 (1), 47–53.
Schmidt, L., Gaikowski, M., Gingerich, W., 2006. Environmental Assessment for the Use of Hydrogen Peroxide in Aquaculture for Treating External Fungal and Bacterial Diseases of Cultured Fish and Fish Eggs Prepared by. Food and Drug Administration's New Animal Drug Application Number, U.S.
Sharrer, M.J., Summerfelt, S.T., Bullock, G.L., Gleason, L.E., Taeuber, J., 2005. Inactivation of bacteria using ultraviolet irradiation in a recirculating salmonid culture system. Aquacult. Eng. 33 (2), 135–149. https://doi.org/10.1016/J.AQUAENG.2004.12.001.
Skrabal, S.A., 2006. Dissolved titanium distributions in the Mid-Atlantic Bight. Mar. Chem. 102 (3–4), 218–229. https://doi.org/10.1016/J.MARCHEM.2006.03.009.
Soltan, M. (2016). Aquaculture systems. Retrieved October 12, 2020, from https://www.researchgate.net/publication/308928410_Aquaculture_systems.
Song, K., Mohseni, M., Taghipour, F., 2016. Application of ultraviolet light-emitting diodes (UV-LEDs) for water disinfection: A review. Water Res. 94, 341–349. https://doi.org/10.1016/J.WATRES.2016.03.003.
Srinivasa Rao, P.S., Yamada, Y., Leung, K.Y., 2003. A major catalase (KatB) that is required for resistance to H2O2 and phagocyte-mediated killing in Edwardsiella tarda. Microbiology 149 (9), 2635–2644. https://doi.org/10.1099/mic.0.26478-0.
Suantika, G., Situmorang, M. L., Kurniawan, J. B., Pratiwi, S. A., Aditiawati, P., Astuti, D. I., … Simatupang, T. M. (2018). Development of a zero water discharge (ZWD)—Recirculating aquaculture system (RAS) hybrid system for super intensive white shrimp (Litopenaeus vannamei) culture under low salinity conditions and its industrial trial in commercial shrimp urban farming in G. Aquacultural Engineering, 82(December 2017), 12–24. https://doi.org/10.1016/j.aquaeng.2018.04.002.
Summerfelt, S.T., Sharrer, M.J., Tsukuda, S.M., Gearheart, M., 2009. Process requirements for achieving full-flow disinfection of recirculating water using ozonation and UV irradiation. Aquacult. Eng. 40 (1), 17–27. https://doi.org/10.1016/j.aquaeng.2008.10.002.
Thayanukul, P., Kurisu, F., Kasuga, I., Furumai, H., 2013. Evaluation of microbial regrowth potential by assimilable organic carbon in various reclaimed water and distribution systems. Water Res. 47 (1), 225–232. https://doi.org/10.1016/j.watres.2012.09.051.
Torgersen, Y., Håstein, T., 1995. Disinfection in aquaculture. Revue Scientifique et Technique (International Office of Epizootics) 14 (2), 419–434. https://doi.org/10.20506/rst.14.2.845.
Villar-Navarro, E., Levchuk, I., Rueda-Márquez, J.J., Manzano, M., 2019. Combination of solar disinfection (SODIS) with H2O2 for enhanced disinfection of marine aquaculture effluents. Sol. Energy 177, 144–154. https://doi.org/10.1016/j.solener.2018.11.018.
Vivar, M., Pichel, N., Fuentes, M., López-Vargas, A., 2017. Separating the UV and thermal components during real-time solar disinfection experiments: The effect of temperature. Sol. Energy 146, 334–341. https://doi.org/10.1016/j.solener.2017.02.053.
Walczak, M., Swiontek Brzezinska, M., 2009. The impact of UV mediated hydrogen peroxide on culturable bacteria in the surface microlayer of eutrophic lake. Polish Journal of Ecology 57 (3), 547–554.
Yan, L., Stallard, R.F., Key, R.M., Crerar, D.A., 1991. Trace metals and dissolved organic carbon in estuaries and offshore waters of New Jersey, USA. Geochim. Cosmochim. Acta 55 (12), 3647–3656. https://doi.org/10.1016/0016-7037(91)90062-A.
Yokoi, K., van den Berg, C.M.G., 1991. Determination of titanium in sea water using catalytic cathodic stripping voltammetry. Anal. Chim. Acta 245 (C), 167–176. https://doi.org/10.1016/S0003-2670(00)80217-2.
You, J., Guo, Y., Guo, R., Liu, X., 2019. A review of visible light-active photocatalysts for water disinfection: Features and prospects. Chem. Eng. J. 373 (May), 624–641. https://doi.org/10.1016/j.cej.2019.05.071.
Zepeda-Velázquez, A.P., Vega-Sánchez, V., Ortega-Santana, C., Rubio-Godoy, M., de Oca-Mira, D.M., Soriano-Vargas, E., 2017. Pathogenicity of Mexican isolates of Aeromonas sp. in immersion experimentally-infected rainbow trout (Oncorhynchus mykiss, Walbaum 1792). Acta Trop. 169, 122–124. https://doi.org/10.1016/J.ACTATROPICA.2017.02.013.
Zhang, Y., Sivakumar, M., Yang, S., Enever, K., Ramezanianpour, M., 2018. Application of solar energy in water treatment processes: A review. Desalination 428, 116–145. https://doi.org/10.1016/J.DESAL.2017.11.020.